Sensors and Actuators B 134 (2008) 761–768

Contents lists available at ScienceDirect

Sensors and Actuators B: Chemical

journal homepage: www.elsevier.com/locate/snb

Synthesis of flower-like CuO nanostructures as a sensitive sensor for catalysis

Fei Teng[a,b,*], Wenqing Yao[b], Youfei Zheng[a], Yutao Ma[c], Yang Teng[d], Tongguang Xu[b], Shuhui Liang[b], Yongfa Zhu[b,**]

[a] Department of Chemistry, Nanjing University of Information Science & Technology, Nanjing 210044, PR China
[b] Department of Chemistry, Tsinghua University, Beijing 100084, PR China
[c] School of Science, Beijing Jiaotong University, Beijing 100044, PR China
[d] Department of Information Science, Suzhou Institute of Trade & Commerce, Suzhou 215009, PR China

ARTICLE INFO

Article history:
Received 2 April 2008
Received in revised form 14 June 2008
Accepted 16 June 2008
Available online 25 June 2008

Keywords:
CuO
Flower-like
Hydrothermal
Chemiluminescence
CO oxidation

ABSTRACT

The flower-like CuO nanostructures were hydrothermally synthesized without using any template. The influences of hydrothermal temperature and time on the growth of nanostructures were investigated. The samples were characterized by means of scanning electron microscope (SEM), X-ray powder diffraction (XRD), transmission electron microscope (TEM), high-resolution transmission electron microscope (HRTEM), selected area electron diffraction (ED), and N_2 adsorption isotherm. Interestingly, these architectures are made of three-order structures. The formation mechanism of the flower-like CuO was proposed and explained. Furthermore, the chemiluminescence (CL) and catalysis properties of the flower-like CuO were also investigated. The flower-like nanostructures showed the high-CL intensities and reactive activities for CO oxidation. The flower-like CuO can be used to fabricate a highly sensitive CL detector. This CL mode is a rapid and effective method for the selection of new catalysts from thousands of materials.

1. Introduction

Recently, the research on the shape control of various nanostructures has been widely developed because of their morphology dependent properties. The cuprous oxide (Cu_2O) and copper oxide (CuO) with different morphologies have also been prepared by several routes, such as thermal oxidation [1], simple solution [2], simple hydrolysis [3], template-based sol–gel [4], and electrochemical [5]. Besides, the hydrothermal [6–10], solvothermal [11,12] and microwave-hydrothermal [13,14] methods have also been employed to control the morphologies of these oxides. Furthermore, it has been shown that the addition of different surfactants can effectively promote the formation of CuO/Cu_2O nanostructures (2D and 3D) [15–18].

CuO is a p-type semiconductor with a narrow bandgap (1.2 eV), which shows the interesting electrochemical and catalytic properties. CuO has received considerable attention due to its potential applications in many fields, such as catalysis, gas sensors, and superconductors [19–21]. The advanced structures of CuO with varied shapes have been obtained, such as nanowires, nanoribbons, hollow, dendrites, dandelions, pricky, flowers and film [22–32]. Liu and Zeng [27] have reported the self-organization of CuO hierarchical microspheres. The microspheres are similar to the spherical assemblies or "dandelions" with a puffy appearance. Xu et al. [28] have also prepared CuO pricky microspheres using a simple solution method. Besides, CuO whisker assemblies have also been synthesized by a microwave-induced process [33]. CuO is an excellent catalyst for CO oxidation, which has been widely used in indoor air cleaning, fuel cells and automotive exhaust treatment [34–36]. It is important to explore oxide-based hierarchical structures for the applications in catalysis and nanodevices. To the best of our knowledge, however, the majorities of researches mainly focus on the synthesis of these advanced micro-/nanostructures; the physico-chemistry properties of these advanced structures have been scarcely reported.

In this work, the flower-like CuO nanostructure was hydrothermally synthesized using copper threads as precursor. The influences of hydrothermal temperature and time on the growth of crystals were investigated, and the formation mechanism of CuO nanostructure was proposed and discussed. The chemiluminescence (CL) and catalysis properties of the samples were investigated. Furthermore, a highly sensitive CL detector was fabricated using these nanostructures.

* Corresponding author at: Department of Chemistry, Nanjing University of Information Science & Technology, 114# Pancheng, Pukou, Nanjing 210044, PR China. Tel.: +86 25 5873 6689; fax: +86 10 6278 7601.
** Corresponding author. Tel.: +86 25 5873 6689; fax: +86 10 6278 7601.
E-mail addresses: tfwd@163.com (F. Teng), zhuyf@mail.tsinghua.edu.cn (Y. Zhu).

0925-4005/$ – see front matter © 2008 Elsevier B.V. All rights reserved.
doi:10.1016/j.snb.2008.06.023

Table 1
Preparation, surface areas, crystal structures, CL intensities, and catalytic activities of the samples

Sample	T (°C), time (h)	S_{BET} ($m^2\ g^{-1}$)[a]	CL intensity ($\times 10^4$ a.u.)	T_{50} (°C)[b]	Crystal structure
S1	100, 24	–	–	–	$Cu(OH)_2$
S2	120, 24	15.5	1.6	160	CuO
S3	140, 2	–	–	–	$Cu(OH)_2$
S4	140, 8	14.5	2.0	155	CuO
S5	140, 12	10.3	2.5	150	CuO
S6	140, 24	9.7	2.8	145	CuO
S7	160, 24	9.2	3.1	140	CuO
S8	180, 24	8.4	3.7	130	$CuO + Cu_2O$

[a] S_{BET}, surface area calculated by the BET method.
[b] T_{50}, temperature at 50% CO conversion.

2. Experimental procedure

2.1. Synthesis

In the experiments, all chemicals were analytic grade and purchased from Beijing Chemicals Company of China. They were used without further purification.

Typically, the copper threads (99.99%, 10 mm × 1 mm) were immersed in a 2.0 M HCl solution under ultrasonic stirring; after 10 min, the copper threads were washed with acetone and deionized water in sequence to remove the surface impurities. 1.0 g of the fresh copper threads was put into a 50-mL Teflon-lined autoclave containing 40 mL of 0.5 mol L^{-1} $K_2Cr_2O_7$ and 5 mL of 98 wt.% H_2SO_4 solutions, while the pH value of the solution was kept at 2–3. The autoclave was then sealed and heated to 140 °C in an oven.

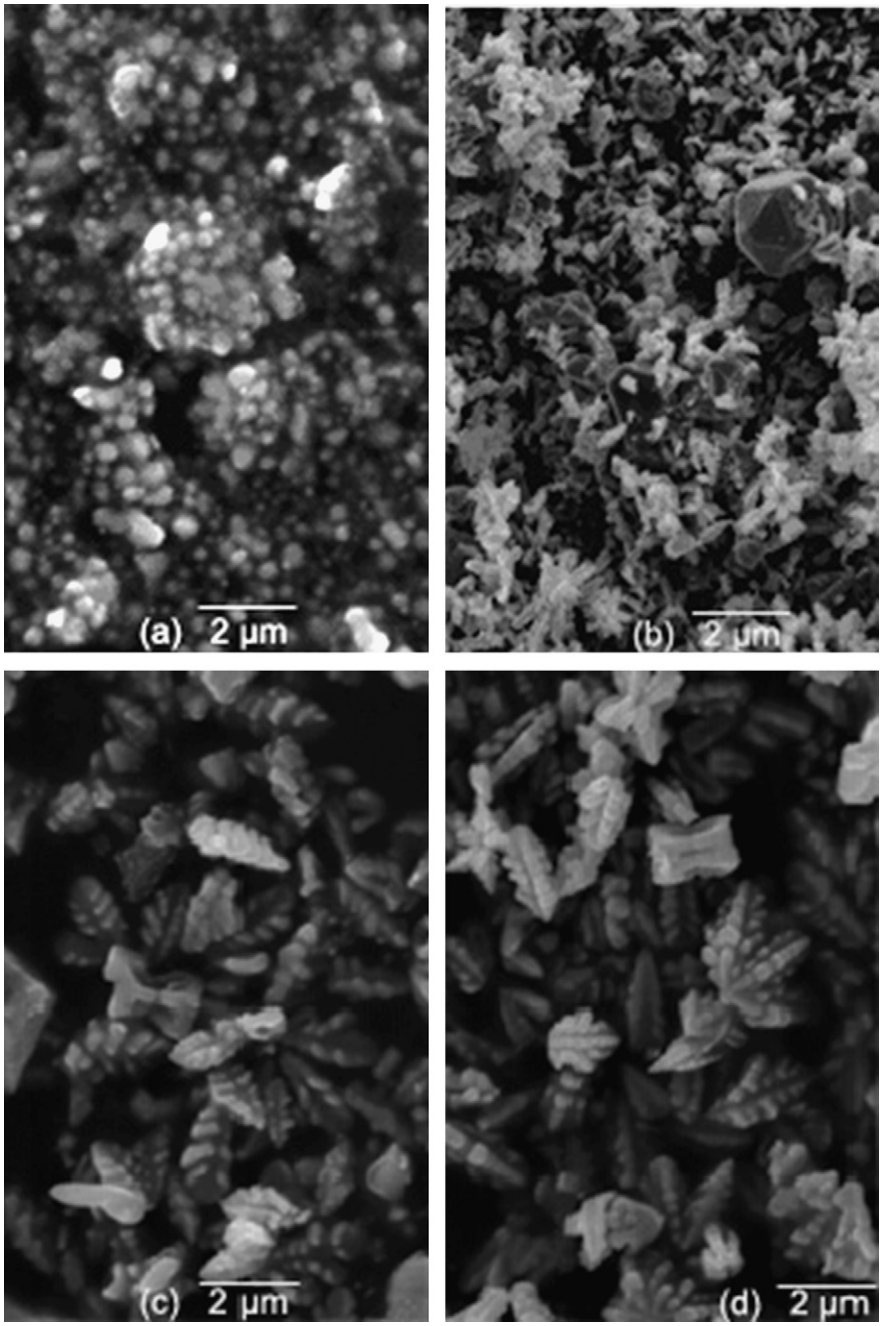

Fig. 1. SEM micrographs of the samples prepared at different reaction temperatures for 24 h: (a) T = 100 °C, (b) T = 120 °C, (c) T = 140 °C, and (d) T = 160 °C.

After 24 h, the remained copper threads were taken out from the mixture. The solids were separated by centrifugation, washed with deionized water, and dried at 80 °C overnight. In order to explore the formation of the nanostructures, the hydrothermal temperature and time were varied, respectively.

2.2. Characterization

The morphologies of the samples were characterized by a scanning electron microscope (SEM, KYKY 2800) equipped with a Link ISIS EDS analyzer. The acceleration voltage was 15 keV and the current was 1.2 nA. The morphologies of the samples were also observed on a transmission electron microscope (TEM, JEOL 200CX) with an accelerating voltage of 200 kV. High-resolution transmission electron microscope (HRTEM, JEOL JEM-2010) was used to characterize the surface structures of the samples. The powders were ultrasonically dispersed in ethanol, and then deposited on a thin amorphous carbon film supported by a copper grid. The crystal structures of the samples were characterized by X-ray powder diffractometer (XRD, Rigaku D/MAX-RB), using graphite monochromatized Cu Kα radiation ($\lambda = 0.154$ nm), operating at 40 kV and 50 mA. The XRD patterns were obtained in the range of 10–70° (2θ) at a scanning rate of 5 ° min^{-1}. A nitrogen adsorption isotherm was performed at −196 °C on a Micromeritics ASAP2010 gas adsorption analyzer. The sample was degassed at 200 °C for 3 h before the measurement. The surface area was calculated by the Brunauer–Emmett–Teller BET method [37].

2.3. Evaluation of chemiluminescence and catalytic properties

CL properties were evaluated on a CL detection system, which is made by Biophysics Institute of Chinese Academy of Science in China. The powders were sintered to form a 0.2-mm thickness coating on the heating tube. The sensor was put into a quartz tube with the inner diameter of 12 mm. The mixed gases of air and CO flowed through the quartz tube at a rate of 100 mL min^{-1}, and CO concentration in the mixed gases was kept at 400 μg mL^{-1}. The bandpass filter of 425-nm band length was used. The resulting CL signal at 200 °C was directly measured with a BPCL ultra-weak luminescence analyzer.

The oxidation reaction of CO was carried out in a conventional flow system at an atmospheric pressure. 0.1 g of the catalyst was loaded in a quartz reactor (inner diameter: 5 mm), with quartz beads packed at both ends of the catalyst bed. The thermal couple was inserted in the catalyst bed to monitor the reaction temperature since CO oxidation is an exothermic reaction. Before each run, the catalyst bed was flushed with air (100 mL min^{-1}) at 300 °C for 1 h, so as to remove the adsorbed species from the catalyst surface, and then cooled to 30 °C. The mixed gases of 2 vol.% CO and 98 vol.% air were fed to the catalyst bed at a certain flowing rate of 100 mL min^{-1}. The inlet and outlet gas compositions were analyzed by an on-line gas chromatograph with a GDX-403 GC-column (1.5 m × 4 mm) and a hydrogen flame ionization detector (FID).

3. Results and discussion

3.1. Formation and characterization of the nanostructures

Table 1 gives the preparation conditions of the samples. In order to investigate the influence of hydrothermal temperature on the nanostructures, the samples were prepared at 100, 120, 140, 160, and 180 °C for 24 h, respectively. Their typical SEM micrographs and XRD patterns are shown in Figs. 1 and 2, respectively. At 100 °C, a large number of the nanoparticles were prepared

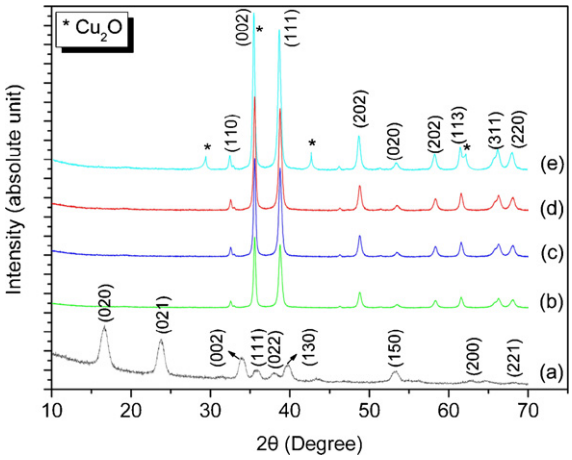

Fig. 2. XRD patterns of the samples prepared at different reaction temperatures for 24 h: (a) $T = 100$ °C, (b) $T = 120$ °C, (c) $T = 140$ °C, (d) $T = 160$ °C, and (e) $T = 180$ °C.

(Fig. 1(a)). All the diffraction peaks of the sample could be indexed to an orthorhombic structure of $Cu(OH)_2$ with the lattice constants $a = 2.951$ Å, $b = 10.59$ Å and $c = 5.273$ Å (JCPDS 35-0505) (Fig. 2(a)). This is also confirmed by the color of the product (the characteristic blue color of $Cu(OH)_2$). This indicates that CuO crystals cannot be formed due to the low temperature. When the temperature was increased to 120 °C, both small flowers and nanoparticles were obtained (Fig. 1(b)). At 140 and 160 °C, a large number of the well-organized flower-like structures were obtained (Fig. 1(c) and (d)). Interestingly, many of crystal ornaments can be clearly observed on the petals. All the diffraction peaks of the samples can be indexed to a monoclinic structure of CuO with the lattice constants $a = 4.6837$ Å, $b = 3.4226$ Å and $c = 5.1288$ Å (JCPDS 45-0937) (Fig. 2(b)–(d)). At 180 °C, the flower-like structures have not been prepared, but the irregular particles formed (not showing the SEM micrographs). Fig. 2(e) shows that this sample consists of CuO and a small amount of Cu_2O. The formation of Cu_2O can be also confirmed by the reddish color of the product. This result indicates that Cu(II) can be reduced to Cu(I) at a high-hydrothermal temperature. The result is well consistent with the reports by other researchers [38,39]. It is obvious that the hydrothermal temperature has a significant influence on the morphology and structure of the product. In this study, the well-organized CuO flower-like nanostructures could form at 140–160 °C.

To explore the formation of the nanostructures, the hydrothermal time was varied from 2, 8, 12, to 24 h while the hydrothermal temperature was kept at 140 °C. After 2 h, a large number of nanoparticles were formed (Fig. 3(a)). When the reaction time was prolonged to 8 h, the small flowers formed, and the lengths of the petals are about 1.5–2 μm (Fig. 3(b)). After 12 h, the well-organized flower-like architectures formed, and the lengths of the petals reached 2.5–3 μm (Fig. 3(c)). After 24 h, the sample has a three-order structure, and the lengths of the petals were about 4–5 μm (Fig. 3(d)). The crystal ornaments can be clearly observed on the petals. Further prolonging the reaction time, the sizes of the flowers did not increase significantly. Fig. 4 shows the XRD patterns of the as-synthesized samples at 140 °C. After 2 h, the sample shows the structure of $Cu(OH)_2$ (Fig. 4(a)). When the reaction time was prolonged to 8, 12, and 24 h, all the samples showed the crystal structure of CuO (Fig. 4(b)–(d)). No Cu_2O or $Cu(OH)_2$ could be detected by XRD. It is obvious that the reaction time has also a significant influence on the morphology and structure of the products. It seems that the flower-like structures may grow from the nanoparticles.

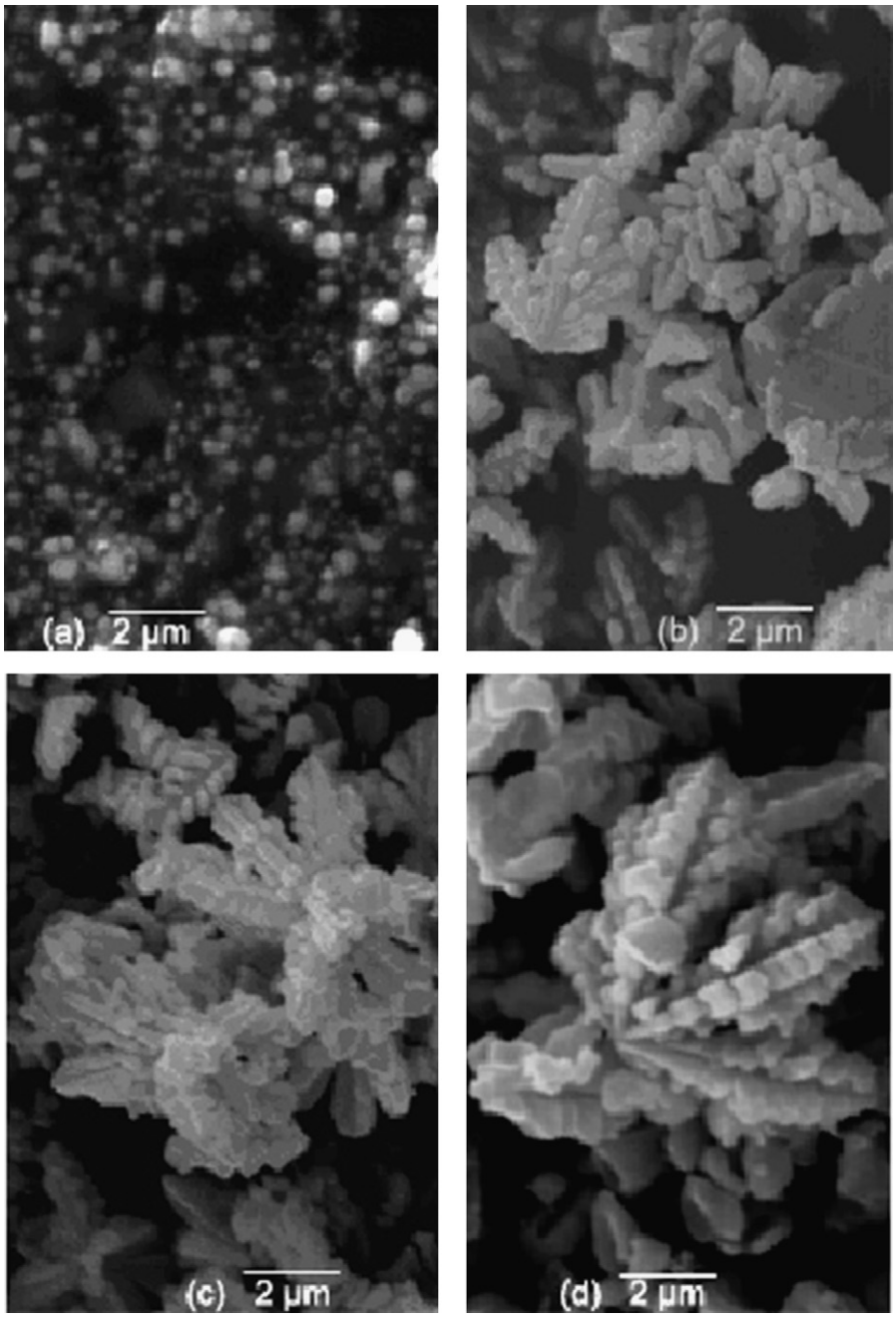

Fig. 3. SEM micrographs of the samples prepared at 140 °C for different reaction intervals: (a) $t = 2$ h, (b) $t = 8$ h, (c) $t = 12$ h, and (d) $t = 24$ h.

Further, the sample (in Fig. 3(d)) was characterized by TEM, HRTEM and ED. Fig. 5(a) and (b) show the typical TEM micrographs of the flowers with several petals. Fig. 5(c) shows the typical TEM image of a petal. It reveals that the flower-like structure is made of the three-order structure: the nanocrystals, the petals, and the assembly of the petals. Fig. 5(d) shows the typical HRTEM image of the ornament (indicated by the arrow in Fig. 5(c)). The interplanar spacings were estimated to be 0.215, 0.232, and 0.274 nm, which correspond to the [0 0 2], [1 1 1], and [1 1 0] planes of a monoclinic CuO crystal, respectively. Fig. 5(e) shows the ED pattern of the ornament (indicated by the arrow in Fig. 5(c)). The diffraction rings could be also indexed to a monoclinic CuO structure, rather than a cubic Cu_2O structure. The diffraction rings confirm the polycrystalline properties of the sample.

Based on the observations, the oxidation-dehydration processes may have occurred as below:

$$3Cu + Cr_2O_7^{2-} + 8H^+ \rightarrow 3Cu(OH)_2 + 2Cr^{3+} + H_2O \quad (1)$$

$$Cu(OH)_2 \rightarrow CuO + H_2O \quad (2)$$

The $Cr_2O_7^{2-}$ ions have the high-oxidation potential in the slightly acidic solution, the redox reaction could occur between $Cr_2O_7^{2-}$ and Cu. The $Cr_2O_7^{2-}$ ions moved and attacked the surfaces of Cu threads, and Cu (0) was oxidized to form Cu(II) ion; at the same time, the pH value of the solution would increase slightly, resulting in the formation of $Cu(OH)_2$ nanocrystals. Under the hydrothermal conditions, $Cu(OH)_2$ could be transformed into CuO through a dehydration/dehydroxylation process. The reaction

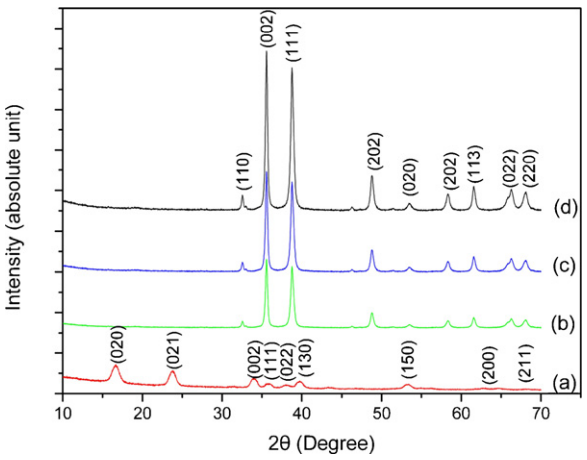

Fig. 4. XRD patterns of the samples prepared at 140 °C for different reaction intervals: (a) $t = 2$ h, (b) $t = 8$ h, (c) $t = 12$ h, and (d) $t = 24$ h.

process can be also confirmed by the surface variation of Cu thread before and after reaction (Fig. 6). Before reaction, the surface of Cu thread was glazed; after reaction, however, Cu thread was eroded and the surface became concave. At 140 °C, the variation of the petal size with hydrothermal time was followed by SEM (Fig. 7). Before 4 h, the petal size increased slowly, indicating that the nucleation of the crystals is significant; in the range of 5–16 h, the petal size increased quickly, indicating that the growth of crystals is significant; after 16 h, the petal size did not increase significantly. This may imply that the petals likely may result from the growth of the primary nanocrystals. In the process, the small crystals grew into the petals through an Oswald ripening process. Since Cu threads were used as the precursor, we could picture that Cu solid may also provide the specific heterogeneous nucleation sites and initiate the growth of the crystals, in which the flower-like structures may have formed via a solid-solution-solid process [40–42]. With the proceeding of the reaction, the pH value of the solution increased slightly, which in turn promoted the formation of $Cu(OH)_2$ or CuO crystals. Cu thread, providing with the specific sites, facilitated the nucleation and growth of $Cu(OH)_2$ or CuO crystals; CuO crystals further grew into the petals; thereafter, the petals may fuse "head-to-head" into the flower-like structures while Cu threads were completely oxidized. Similar to the report by Zeng and co-workers [43], the needlelike branches can fuse side-by-side into each other.

Hydrothermal reaction is an effective method to obtain the desirable crystals, such as mild conditions, controllable morphology, low aggregation and high crystallinity. It could be assumed that the formation of the flower-like structure was controlled not only by the growth thermodynamics, but also by the growth kinetics. The formation process could be purposely divided into several processes: (i) formation of the primary nanocrystals, (ii) growth of the secondary structure and (iii) formation of the three-order structure. The growth mechanism is similar to those of the branched ZnO [43] and Cu_2O crystals [44]. Fig. 8 was used to illustrate the formation of the flower-like structures. While Cu was oxidized by $K_2Cr_2O_7$, $Cu(OH)_2$ or CuO nanocrystals formed and adsorbed on the surface of Cu thread (Fig. 8(a)); these nanocrystals grew into the pristine petals through the dissolution/crystallization process, and the small petals further grew into the large ones (Fig. 8(b)). At the same time, the nanocrystals grew on these petals and formed the small ornaments (Fig. 8(c)). It seems that the nucleation and growth of the crystals could be promoted by Cu solids. While Cu threads were

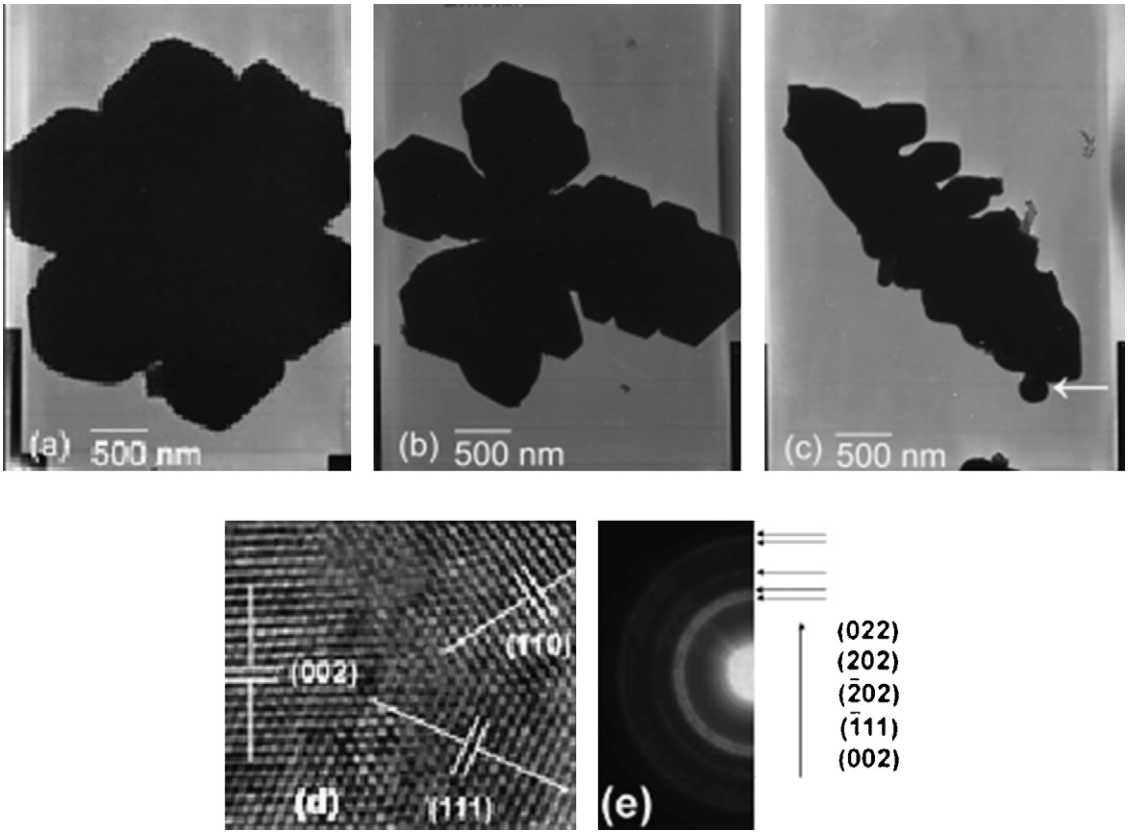

Fig. 5. TEM, HRTEM micrographs and ED pattern of the CuO flowers prepared at 140 °C for 24 h: (a–c) TEM, (d) HRTEM, and (e) ED.

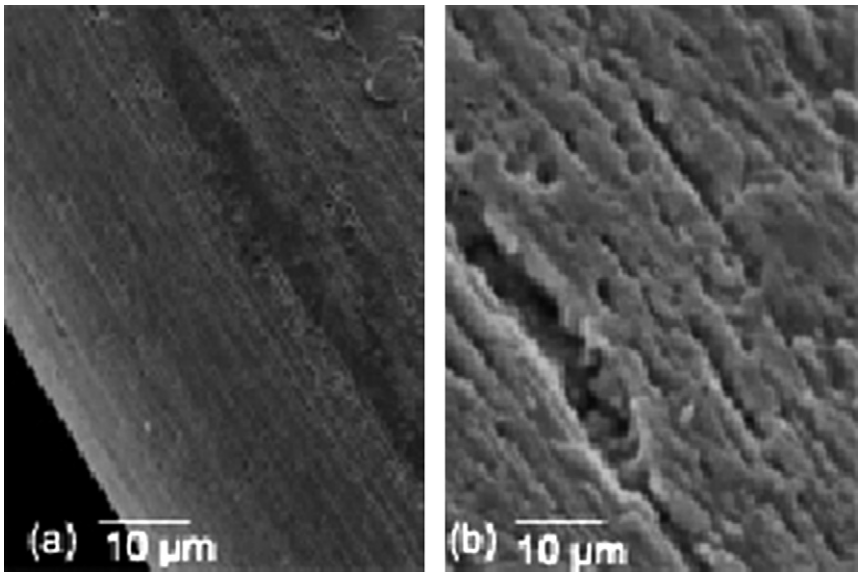

Fig. 6. SEM micrographs of the Cu thread before (a) and after (b) reaction at 140 °C for 2 h.

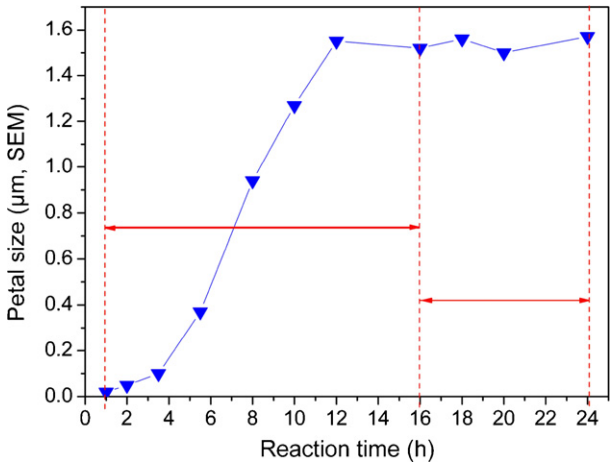

Fig. 7. The petal sizes of the CuO flowers prepared at 140 °C for different intervals: the petal sizes were obtained by SEM.

oxidized completely, the petals may fuse "head-to-head" to form the flower-like structures. Note that the formation of the nanostructures and the phase transformation of $Cu(OH)_2$ into CuO have occurred simultaneously. To clearly picture what truly governs the site-specific nucleation and growth as such, our extensive studies including interface spectroscopic analysis and computational simulation are ongoing currently.

3.2. Chemiluminescence (CL) and catalysis properties of the nanostructures

Since CuO is an excellent oxidation catalyst for CO oxidation, the CL and catalysis properties of the flower-like CuO nanostructures were studied. Fig. 9 shows the CL spectra of CO oxidation over the catalysts. Herein, the catalysts synthesized at 120/24, 140/8, 140/12, 140/24, 160/24, and 180/24 (°C/h) were designated as S2, S4, S5, S6, S7, and S8, respectively. It could be observed that the CL intensities of the catalysts follow the orders: S2 (1.6×10^4 a.u.) < S4 (2.0×10^4 a.u.) < S5 (2.5×10^4 a.u.) < S6 (2.8×10^4 a.u.) < S7 (3.1×10^4 a.u.) < S8 (3.7×10^4 a.u.). This indicates that the different amounts of the CO_2 molecules may be

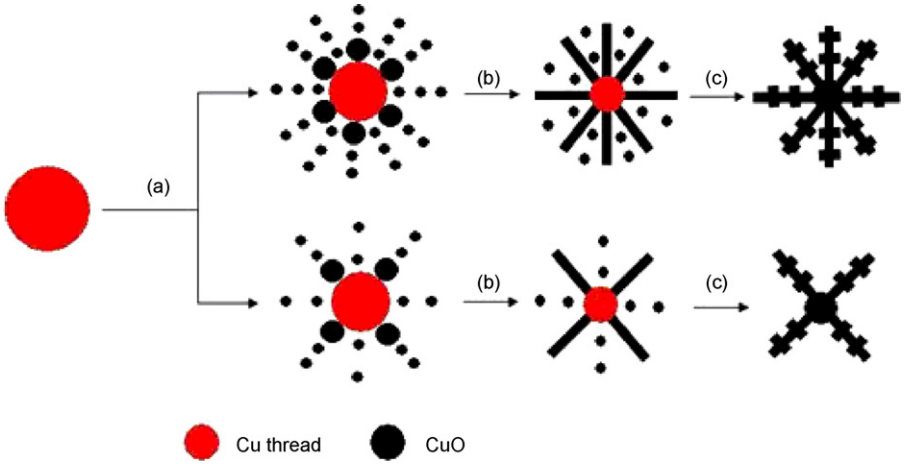

Fig. 8. The formation sketch diagram of the flower-like structures: (a) formation of nanocrystals, (b) growth of the petals, and (c) growth of small ornaments formation of the flower structures.

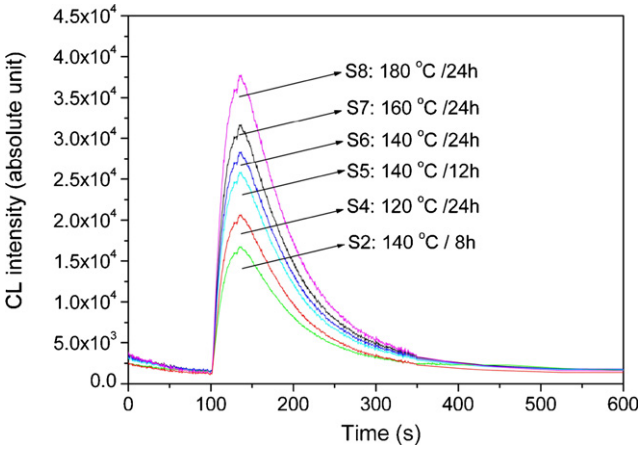

Fig. 9. The CL spectra of CO oxidation over the catalysts synthesized under different conditions. Test conditions of the CL spectra: $T = 200\,^{\circ}C$, 400 μg mL^{-1} CO, 100 mL min^{-1} of flow rate (CO + air).

produced. It is generally accepted that the CL reaction can be represented with the following equations [45,46]:

$$CO(ads) + O \rightarrow CO_2(ads) + Energy \rightarrow CO_2^*(ads) \rightarrow CO_2 + h\nu$$

While the CO molecules were oxidized on the solid surface, an amount of energy was released, which would be absorbed by the produced CO_2 molecules. As a result, the CO_2 molecules would jump from the electronic ground state to the electronic excited state (CO_2^*). While the electronic excited CO_2^* molecules decayed to the electronic ground state, a weak light would be emitted. The CL intensity is linearly proportional to the produced CO_2 concentration [46]. The CL intensity may closely correlate with the catalytic reaction.

Further, the reaction activities of CO oxidation over these catalysts were also evaluated. Their activities are shown in Fig. 10 and summarized in Table 1. The temperatures at 50% CO conversion (T_{50}) over S2, S4, S5, S6, S7, and S8 are 160, 155, 150, 145, 140, and 130 °C, respectively. The XRD results showed that the crystallinities of the catalysts follows the orders: S2 < S4 < S5 < S6 < S7 < S8; however, the BET areas of the catalysts follow the orders: S2 (15.5 m g^{-1}) > S4 (14.5 m g^{-1}) > S5 (10.3 m g^{-1}) > S6 (9.7 m g^{-1}) > S7 (9.2 m g^{-1}) > S8 (8.4 m g^{-1}). The results mean that the crystallinity of the catalyst played the dominating role in the catalytic oxidation of CO, but the BET area played the minor role. The amounts of amorphous form present in the low-crystallinity catalyst may not favor for the oxidation of CO. As a result, the high-crystallinity catalyst showed a high-catalytic activity. The highest activity of the S8 sample could be ascribed to the high crystallinity and the presence of Cu_2O. It has been reported that Cu_2O had a higher activity of CO oxidation than CuO crystal [47]. It is most important that the order of the CL intensities of the catalysts is well consistent to that of their reaction activities. The CL spectra could be used to quantitatively evaluate a given catalytic reaction.

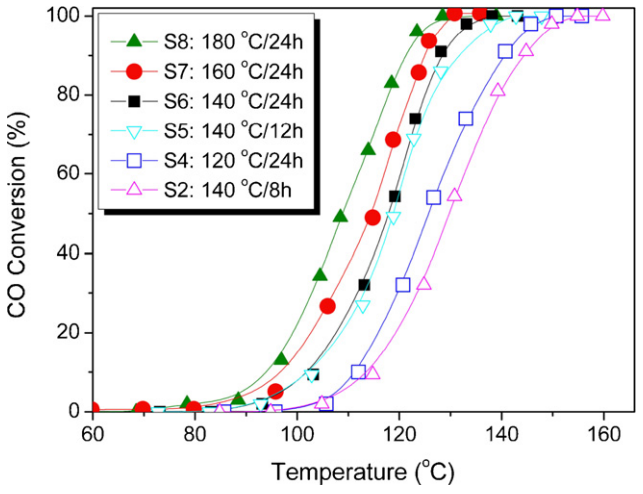

Fig. 10. The activities of the catalysts for CO oxidation. Test conditions of the activities: 100 mL min^{-1} of flow rate (CO + air), 2 vol.% CO, 98 vol.% air.

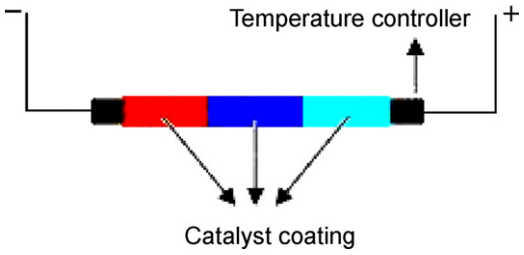

Fig. 11. Scheme diagram of the CL sensor.

Based on the good correlation between CL intensity and activity, we have developed a CL-based detector with the multi-regions (Fig. 11). This technique could be potentially applied to explore the new catalysts. The different catalysts can be coated on the different regions, and the CL signals can be acquired by adjusting the location of the coating. The multi-region CL detector is simple and rapid for screening the catalysts. It is known that the catalyst evaluation is generally performed by testing the reaction activity, in which the expensive equipment is needed and the test time is long; therefore, the conventional selection mode is expensive, time-consuming and laborious. For the CL mode, no complicate and expensive equipment is needed and the CL spectra can be determined within a few minutes; therefore, the CL mode is facile, rapid, and low cost. It should be noted that the present CL method is effective for judging activity, while possibly insufficient for judging selectivity, which needs further research.

4. Conclusions

The flower-like CuO nanostructures can be hydrothermally synthesized at 120–160 °C for 12–24 h. A highly sensitive CL sensor could be fabricated using the flower-like nanostructures, basing on the close correlation of CL intensity with reaction activity of the catalyst. This CL mode could be facile and effective for screening the excellent catalyst from thousands of materials. It is important to explore oxide-based hierarchical structures for applications in nanodevices.

Acknowledgements

This work is supported financially by National Basic Research Program of China (2007CB613303) and Chinese Postdoctoral Science Foundation (no. 20060390057).

References

[1] J.T. Chen, F. Zhang, J. Wang, G.A. Zhang, B.B. Miao, X.Y. Fan, D. Yan, P.X. Yan, CuO nanowires synthesized by thermal oxidation route, J. Alloys Compd. 454 (2008) 268–273.
[2] L. Yu, G. Zhang, Y. Wu, X. Bai, D. Guo, Cupric oxide nanoflowers synthesized with a simple solution route and their field emission, J. Cryst. Growth 310 (2008) 3125–3130.
[3] J. Zhu, H. Bi, Y. Wang, X. Wang, X. Yang, L. Lu, Synthesis of flower-like CuO nanostructures via a simple hydrolysis route, Mater. Lett. 61 (2007) 5236–5238.

[4] Y.-K. Su, C.-M. Shen, H.-T. Yang, H.-L. Li, H.-J. Gao, Controlled synthesis of highly ordered CuO nanowire arrays by template-based sol–gel route, Trans. Nonferrous Met. Soc. China 17 (2007) 783–786.
[5] G.-Q. Yuan, H.-F. Jiang, C. Lin, S.-J. Liao, Shape- and size-controlled electrochemical synthesis of cupric oxide nanocrystals, J. Cryst. Growth 303 (2007) 400–406.
[6] H. Zhang, S. Li, X. Ma, D. Yang, Controllable growth of dendrite-like CuO nanostructures by ethylene glycol assisted hydrothermal process, Mater. Res. Bull. 43 (2008) 1291–1296.
[7] M. Zhang, X. Xu, M. Zhang, Hydrothermal synthesis of sheaf-like CuO via ionic liquids, Mater. Lett. 62 (2008) 385–388.
[8] M.-G. Ma, Y.-J. Zhu, Hydrothermal synthesis of cuprous oxide microstructures assembled from needles, J. Alloys Compd. 455 (2008) L15–L18.
[9] Z.-Z. Chen, E.-W. Shi, Y.-Q. Zheng, W.-J. Li, B. Xiao, J.-Y. Zhuang, Growth of hexpod-like Cu_2O whisker under hydrothermal conditions, J. Cryst. Growth 249 (2003) 294–300.
[10] Y.C. Zhang, J.Y. Tang, G.L. Wang, M. Zhang, X.Y. Hu, Facile synthesis of submicron Cu_2O and CuO crystallites from a solid metallorganic molecular precursor, J. Cryst. Growth 294 (2006) 278–282.
[11] X.-L. Tang, L. Ren, L.-N. Sun, W.-G. Tian, M.-H. Cao, C.-W. Hu, A solvothermal route to Cu_2O nanocubes and Cu nanoparticles, Chem. Res. Chin. Univ. 22 (2006) 547–551.
[12] X. Song, H. Yu, S. Sun, Single-crystalline CuO nanobelts fabricated by a convenient route, J. Colloid Interf. Sci. 289 (2005) 588–591.
[13] D. Keyson, D.P. Volanti, L.S. Cavalcante, A.Z. Simões, J.A. Varela, E. Longo, CuO urchin-nanostructures synthesized from a domestic hydrothermal microwave method, Mater. Res. Bull. 43 (2008) 771–775.
[14] X. Xu, M. Zhang, J. Feng, M. Zhang, Shape-controlled synthesis of single-crystalline cupric oxide by microwave heating using an ionic liquid, Mater. Lett. 62 (2008) 2787–2790.
[15] W.-T. Yao, S.-H. Yu, Y. Zhou, J. Jiang, Q.-S. Wu, L. Zhang, J. Jiang, Formation of uniform CuO nanorods by spontaneous aggregation: selective synthesis of CuO, Cu_2O, and Cu nanoparticles by a solid–liquid phase arc discharge process, J. Phys. Chem. B 109 (2005) 14011–14016.
[16] Y. Liu, Y. Chu, M. Li, L. Li, L. Dong, In situ synthesis and assembly of copper oxide nanocrystals on copper foil via a mild hydrothermal process, J. Mater. Chem. 16 (2006) 192–198.
[17] L. Wang, S. Velu, S. Tomora, F. Ohashi, K. Suzuki, M. Okazaki, T. Osaki, M. Maeda, Synthesis and characterization of CuO containing mesoporous silica spheres, J. Mater. Sci. 37 (2002) 801–806.
[18] C.-C. Huang, J.R. Hwu, W.-C. Su, D.-B. Shieh, Y. Tzeng, C.-S. Yeh, Surfactant-assisted hollowing of Cu nanoparticles involving halide-induced corrosion-oxidation processes, Chem. Eur. J. 12 (2006) 3805–3810.
[19] K. Nagase, Y. Zhang, Y. Kodama, J. Kakuta, Dynamic study of the oxidation state of copper in the course of carbon monoxide oxidation over powdered CuO and Cu_2O, J. Catal. 187 (1999) 123–130.
[20] M. Frietsch, F. Zudock, J. Goschnick, M. Bruns, CuO catalytic membrane as selectivity trimmer for metal oxide gas sensors, Sens. Actuat. B 65 (2000) 379–381.
[21] P.C. Dai, H.A. Mook, G. Aeppli, S.M. Hayden, F. Dogan, Resonance as a measure of pairing correlations in the high-T_c superconductor $YBa_2Cu_3O_{6.6}$, Nature 406 (2000) 965–968.
[22] X. Jiang, T. Herricks, Y.N. Xia, CuO nanowires can be synthesized by heating copper substrates in air, NanoLett. 2 (2002) 1333–1338.
[23] M. Kaur, K.P. Muthe, S.K. Despande, S. Choudhury, J.B. Singh, N. Verma, S.K. Gupta, J.V. Yakhmi, Growth and branching of CuO nanowires by thermal oxidation of copper, J. Cryst. Growth 289 (2006) 670–675.
[24] Y. He, A novel solid-stabilized emulsion approach to CuO nanostructured microspheres, Mater. Res. Bull. 42 (2007) 190–195.
[25] C. Yan, D. Xue, General spontaneous ion replacement reaction for the synthesis of micro- and nanostructured metal oxides, J. Phys. Chem. B 110 (2006) 1581–1586.
[26] S. Li, H. Zhang, Y. Ji, D. Yang, CuO nanodendrites synthesized by a novel hydrothermal route, Nanotechnology 15 (2004) 1428–1432.
[27] B. Liu, H.C. Zeng, Mesoscale organization of CuO nanoribbons: formation of "dandelions", J. Am. Chem. Soc. 126 (2004) 8124–8125.
[28] Y. Xu, D. Chen, X. Jiao, Fabrication of CuO pricky microspheres with tunable size by a simple solution route, J. Phys. Chem. B 109 (2005) 13561–13566.
[29] W. Zhang, S. Ding, Z. Yang, A. Liu, Y. Qian, S. Tang, S. Yang, Growth of novel nanostructured copper oxide (CuO) films on copper foil, J. Cryst. Growth 291 (2006) 479–484.
[30] Z. Yang, J. Xu, W. Zhang, A. Liu, S. Tang, Controlled synthesis of CuO nanostructures by a simple solution route, J. Solid State Chem. 180 (2007) 1390–1396.
[31] W. Zhang, X. Wen, S. Yang, Controlled reactions on a copper surface: synthesis and characterization of nanostructured copper compound films, Inorg. Chem. 42 (16) (2003) 5005–5014.
[32] L.S. Huang, S.G. Yang, T. Li, B.X. Gu, Y.W. Du, Y.N. Lu, S.Z. Shi, Preparation of large-scale cupric oxide nanowires by thermal evaporation method, J. Cryst. Growth 260 (2004) 130–135.
[33] W.W. Wang, Y.-J. Zhu, G.-F. Cheng, Y.-H. Huang, Microwave-assisted synthesis of cupric oxide nanosheets and nanowhiskers, Mater. Lett. 60 (2006) 609–612.
[34] J.B. Reitz, E.I. Solomon, Propylene oxidation on copper oxide surfaces: electronic and geometric contributions to reactivity and selectivity, J. Am. Chem. Soc. 120 (1998) 11467–11478.
[35] W. Liu, M.F. Stephanopoulos, Total oxidation of carbon monoxide and methane over transition metal fluorite oxide composite catalysts. I. Catalyst composition and activity, J. Catal. 153 (1995) 304–316.
[36] B. Skarman, T. Nakayama, D. Grandjean, R.E. Benfield, E. Olsson, K. Niihara, L.R. Wallenberg, Morphology and structure of CuO_X/CeO_2 nanocomposite catalysts produced by inert gas condensation: an HREM, EFTEM, XPS, and high-energy diffraction study, Chem. Mater. 14 (2002) 3686–3699.
[37] S. Brunauer, P.H. Emmett, E. Teller, Adsorption of gases in multimolecular layers, J. Am. Chem. Soc. 60 (1938) 309–319.
[38] R.A. Koppel, C. Stocker, A. Baiker, Copper- and silver-zirconia aerogels: preparation, structural properties and catalytic behavior in methanol synthesis from carbon dioxide, J. Catal. 179 (1998) 515–527.
[39] D. Chen, G. Shen, K. Tang, Y. Qian, Large-scale synthesis of CuO shuttle-like crystals via a convenient hydrothermal decomposition route, J. Cryst. Growth 254 (2003) 225–228.
[40] J.H. Zhan, Y. Bando, J.Q. Hu, D. Golberg, K. Kurashima, Fabrication of ZnO nanoplate–nanorod junctions, Small 2 (2006) 62–65.
[41] T.L. Sounart, J. Liu, J.A. Voigt, J.W.P. Hau, E.D. Spoerke, Z.R. Tian, Y.B. Jiang, Sequential nucleation and growth of complex nanostructured films, Adv. Funct. Mater. 16 (2006) 335–344.
[42] T. Zhang, W. Dong, M. Keeter-Brewer, S. Konar, R.N. Njabon, Z.R. Tian, Site-specific nucleation and growth kinetics in hierarchical nanosyntheses of branched ZnO crystallites, J. Am. Chem. Soc. 128 (2006) 10960–10968.
[43] B. Liu, H.C. Zeng, Hydrothermal synthesis of ZnO nanorods in the diameter regime of 50 nm, J. Am. Chem. Soc. 125 (2003) 4430–4431.
[44] H. Zhang, X. Zhang, H. Li, Z. Qu, S. Fan, M. Ji, Hierarchical growth of Cu_2O double-tower-tip-like nanostructures in water/oil microemulsion, Cryst. Growth Des. 7 (2007) 820–824.
[45] M. Breysse, B. Claudel, L. Faure, M. Guenin, R.J.J. Williams, T.J. Wolkenstein, Chemiluminescence during the catalysis of carbon monoxide oxidation on a thoria surface, J. Catal. 45 (1976) 137–144.
[46] X. Wang, N. Na, S. Zhang, Y. Wu, X. Zhang, Rapid screening of gold catalysts by chemiluminescence-based array imaging, J. Am. Chem. Soc. 129 (2007) 6062–6063.
[47] T.-J. Huang, D.-H. Tsai, CO oxidation behavior of copper and copper oxides, Catal. Lett. 87 (2003) 173–178.

Biographies

Fei Teng obtained his doctor's degree in Physical Chemistry from Dalian Institute of Chemical Physics, Chinese Academy of Sciences in 2005. From 2005 to 2007, he was a postdoctoral researcher in Tsinghua University. He has been an associate professor in Physical Chemistry at Nanjing University of Information and Technology from 2007. His research interests include nanostructure, nanosensor, and photocatalysis.

Wenqing Yao obtained her bachelor's degree in Computer Science from Beijing University of Sciences in 1985. She has been a senior engineer in Surface Chemistry at Tsinghua University from 2001. Her research interests include nanodevice and surface science.

Youfei Zheng obtained his doctor's degree in Environmental Chemistry from Nanjing University of Information and Technology in 1998. He has been a professor in Environmental Science at Nanjing University of Information and Technology from 2000. His research interests include environmental science and analysis.

Yutao Ma obtained his doctor's degree in Inorganic Chemistry from Institute of Chemistry, Chinese Academy of Sciences in 2005. He has been an assistant professor in Inorganic Chemistry at Beijing Jiaotong University from 2007. His research interests include nanostructure and nanosensor.

Yang Teng obtained his master's degree in Computer Science from Dalian University of Technology in 2006. He has been an assistant professor in Computer Chemistry at Suzhou Institute of Trade & Commerce from 2006. His research interests include computer chemistry and nanosensor.

Tongguang Xu obtained his doctor's degree in Analytic Chemistry from Tsinghua University in 2007. He has been a postdoctoral researcher in Physical Chemistry at Tsinghua University. His research interests include photocatalysis and nanostructure.

Shuhui Liang obtained his master's degree in Inorganic Chemistry from Nankai University in 2005. Now, she is studying her doctor' degree in Physical Chemistry at Tsinghua University. Her research interests include nanostructure and heterocatalysis.

Yongfa Zhu obtained his doctor's degree in Physical Chemistry from Tsinghua University in 1990. He has been a professor in Physical Chemistry at Tsinghua University from 1995. His research interests include photocatalysis, nanostructure, nanodevice, and environmental chemistry.